

Loose packings of frictional spheres

Greg R. Farrell*, K. Michael Martini, Narayanan Menon†

Department of Physics, University of Massachusetts, Amherst MA 01003, U.S.A.

We have produced loose packings of cohesionless, frictional spheres by sequential deposition of highly-spherical, monodisperse particles through a fluid. By varying the properties of the fluid and the particles, we have identified the Stokes number (St) – rather than the buoyancy of the particles in the fluid – as the parameter controlling the approach to the loose packing limit. The loose packing limit is attained at a threshold value of St at which the kinetic energy of a particle impinging on the packing is fully dissipated by the fluid. Thus, for cohesionless particles, the dynamics of the deposition process, rather than the stability of the static packing, defines the random loose packing limit. We have made direct measurements of the interparticle friction in the fluid, and present an experimental measurement of the loose packing volume fraction, ϕ_{RLP} , as a function of the friction coefficient μ_s .

I. INTRODUCTION

The most elementary characteristic of a disordered sphere packing is the fraction, ϕ , of the total volume occupied by particles. Stable packings of cohesionless, frictional, spheres exist over a broad range of volume fractions[1–4]. The term “random close packed” (RCP) refers to the upper bound ϕ_{RCP} on the volume fraction at which a packing of identical spheres can be prepared without introducing crystalline ordering. Packings of $\phi \approx 0.64$, are consistently achieved in experiments and simulations; this number is insensitive to variations in interparticle forces and to the compaction protocol, however, questions remain as to whether there exists a tight upper bound [5]. The robustness of ϕ_{RCP} has motivated attempts to understand RCP in purely geometric terms[6] or in terms of the statistical mechanics of hard spheres or soft spheres at zero temperature[7–9]. In this article we experimentally explore the *lower* bound on volume fractions of mechanically stable packings of frictional, noncohesive, identical, hard spheres. Specifically, our questions are: does a loose packing limit exist for frictional but cohesionless spheres? Will this loose packing limit depend on the properties of the particle and the preparation protocol or, like the RCP limit, will it be robust to changes in these variables, and possibly admit descriptions in terms of the statistical mechanics of hard spheres[10]?

In the first systematic study of loose packings, Onoda and Liniger [11] sedimented glass spheres in fluids of varying densities ρ_f , approaching the density ρ_s of the sphere. They found that the packing fraction approached an asymptotic “random loose packed” (RLP) value, $\phi_{RLP} = 0.555$, in the limit of vanishing gravitational acceleration in the fluid, $g_f \equiv g(1 - \rho_f/\rho_s) \rightarrow 0$. However, the limit $g_f \rightarrow 0$ conflates two different physical effects, both of which may plausibly lead to lower volume

fractions. The first effect involves the dynamics of assembling the packing: as $g_f \rightarrow 0$, falling spheres reach the packing with less inertia to explore the surface and rearrange their neighbors. This can trap the particles in higher-energy, fluffier packings. A second, distinct, effect concerns the statics of the structure: as neutral buoyancy is approached, more fragile packings may become stable since the gravitational load borne by the packing vanishes relative to weak cohesive forces. Indeed, simulations by Dong *et al.* [12] argue that attractive van der Waals forces are important in stabilizing the packings of Onoda and Liniger at small g_f . Arbitrarily low packing fractions can be attained when attractive interparticle forces are dominant[13], which calls into question the ability to experimentally access an RLP limit for cohesionless spheres.

A key goal of our experiments is to peel apart the distinct effects of fluid properties on the statics and dynamics. Independently controlling the viscosity and density of the fluid allows us to test whether a unique RLP limit is reached as gentle deposition conditions are approached along arbitrary directions in the density–viscosity plane. Approaching the limit of gentle deposition by increasing viscosity while keeping the gravitational load finite allows us to avoid the cohesive regime and test whether a well-defined ϕ_{RLP} exists for noncohesive spheres.

In the absence of friction, the RLP and the RCP limits are believed to coincide[14]. However, as discussed above, stable packings with $\phi < \phi_{RCP}$ are common, with the packing fraction showing some material-dependence [1, 3]. The relevant material property has been conjectured to be surface roughness [4, 11] and is experimentally found to correlate with angle of repose[15]. Thus, the cause of this variability is generally modelled as a friction coefficient. Simulations with friction find the RLP limit to be a systematically decreasing function of friction [16–19] albeit with unexpectedly large values ($\mu \approx 1$) needed to reproduce values seen experimentally[11, 15]. In this work we directly explore ϕ_{RLP} as a function of measured friction coefficient with noncohesive spheres. We emphasize that particle contacts can exert normal and tangential forces, but cannot support tension.

Another goal of our experiments, complementary to

*E-mail: grfarrell@physics.umass.edu

†E-mail: menon@physics.umass.edu

previous work, is to produce packings by the sequential addition of particles, rather than by collective procedures. Recent experiments by Jerkins *et al.* have studied settling following brief pulses of flow in a liquid-fluidized bed[15] arriving at volume fractions similar to those produced by collective sedimentation[11]. Simulations of sedimented packings[16, 17] have studied volume fraction as a function of particle properties such as friction and inelasticity. Other simulations[14, 18] generate disordered packings by collectively relaxing particle configurations as volume, pressure, temperature or particle interactions are smoothly varied. However, packings created by sequential deposition, in which a particle comes to rest at the first mechanically stable location that it encounters, may lead to different packings than those obtained by collective preparation protocols.

In this article we present data on loose sphere packings prepared by the sequential sedimentation of frictional, non-cohesive spheres large enough to eliminate the influence of van der Waals and other attractive forces. By using fluids of varying density and viscosity, we identify the parameter in the deposition process that controls passage to a putative RLP limit. Rather than g_f , this parameter is the Stokes number, $St \equiv (2/9) \rho_s V r / \eta$, where r is the radius of the sphere, V its velocity and η is the dynamic fluid viscosity. We also vary the friction between spheres, both by varying the material and by increasing surface roughness via controlled etching. We find that the packing fraction in the loose packing limit is a function of interparticle friction, the values of which are quite high, a result in qualitative agreement and simulational findings.

II. EXPERIMENTAL METHODS

We prepared mechanically stable packings of monodisperse spheres immersed in fluids, in an hour-glass shaped apparatus (Fig. 1) placed on a vibration-isolation table. Using a variety of fluids (Table I) and spheres (Table II) we formed packings under a wide range of viscosity and buoyancy conditions allowing distinctions to be drawn between the relative merits of different parameters controlling approach to the RLP limit.

Packings were prepared by inverting the hour-glass shaped cell and allowing particles to settle through the fluid under gravity. The hour-glass geometry consists of two conical sections with a cone angle of 60° and base diameter of 24 sphere-diameters ($d = 2r$) connected by a cylindrical neck of $4.2d$ in diameter, which is only as wide as necessary to avoid jamming by arch formation in the neck. The narrow neck allows the passage of only a few particles at a time. (We have also deposited spheres singly by a mechanical dropper, with very similar results to those reported here.) The packing grows as a conical pile at the angle of repose ($\approx 23 - 26^\circ$), which is much smaller than the cone angle of the container, thus eliminating any empty pockets near the walls. The conical

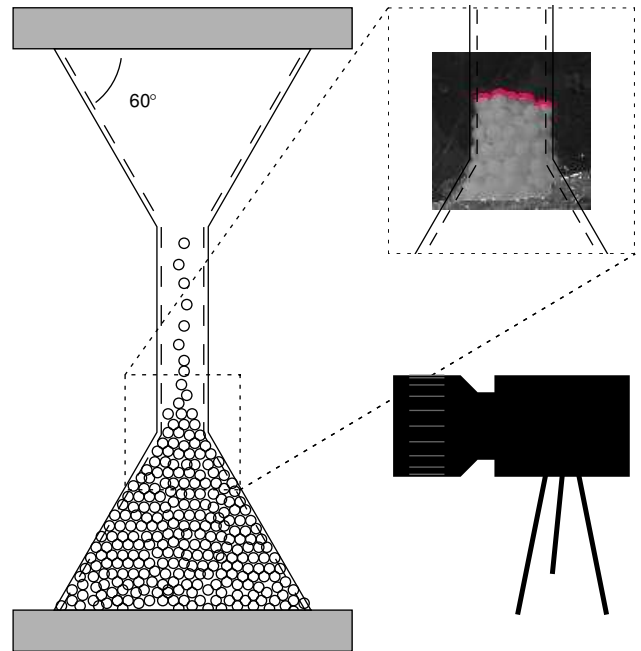


FIG. 1: Hour-glass shaped sedimentation apparatus. Top right: Image of the topography of the top surface of the particles. Since the volume is estimated from a single projection, there is a small systematic positive bias of $\delta\phi \lesssim +0.002$ in measuring the volume of the packing.

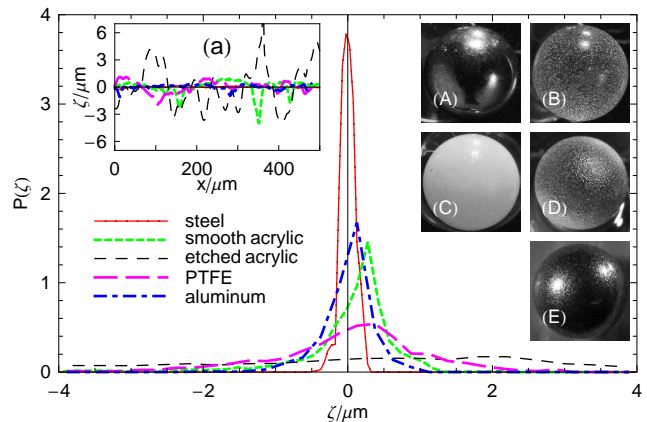


FIG. 2: Histograms of roughness ζ of spherical particles as measured with a Dektak3 profilometer. Inset (a): Select profilometer traces ζ as a function of distance along the surface x (the gross curvature of the sphere has been subtracted). Images of spherical particles: (A) steel, (B) smooth acrylic, (C) PTFE, (D) solvent-etched acrylic, (E) aluminum.

cell was chosen to minimize the weight supported by the sloping walls of the container. No crystalline order was observed near the bottom or side walls.

Data for the volume fraction of the packing are taken when the top surface of the packing just enters the neck of the cell. The total volume of the packing is the volume of the cone plus the small contribution from the spheres

TABLE I: Fluids used in hour-glass sedimentation experiments. The symbols match those used in all figures. Mixture ratios reflect contents before degassing. Density and viscosity were measured after degassing. *lit.[20]. †our measurement. ‡lit. at 20C[20]. §MSDS.

fluid	density/($g\text{ cm}^{-3}$)	viscosity/($mPa\text{ s}$)	symbol
n-pentane (Fisher Sci)	0.626 [†]	0.23*	◀
n-heptane (Fisher Sci)	0.684 [†]	0.41*	▶
water (Millipore)	1.00 [†]	1.03*	▽
n-dodecane (Fisher Sci)	0.75	1.53*	▲
~71/29 n-dodecane/light mineral oil mixture	0.78 [†]	3.02 [†]	○
~50/50 n-dodecane/light mineral oil mixture	0.80 [†]	5.96 [†]	□
~48/52 n-dodecane/light mineral oil mixture	0.82 [†]	11.5 [†]	◆
light mineral oil (Fisher Sci)	0.83 [§]	46.0 [†]	◇
high temperature silicone oil (Acros Organics)	1.05 [§]	117. [†]	●
0.01M NaCl in ~70/30 propylene glycol/glycerol	1.09 [†]	125. [†]	▶
heavy mineral oil (Fisher Sci)	0.83 [§]	157. [†]	◁
Fluka 08577 Density and Viscosity Standard	0.87 [§]	1270. [§]	▼

TABLE II: Properties of sets of spheres. We measured particle diameter using a technique similar to Scott’s[4], measuring the length of ~ 100 spheres in a groove. Density was calculated from this diameter and the weight of these spheres. To quantify polydispersity and sphericity, we measured the diameter of individual spheres with a machinist’s micrometer accurate to $2.5\mu m$, along five or more directions. “Asphericity” is the relative deviation from sphericity calculated as the standard deviation of these diameter measurements relative to the mean. “Polydispersity” is the standard deviation of the average diameters of a set of 20 spheres relative to the mean. “RMS roughness” gives the root-mean-square deviation from sphericity of profilometer traces taken of the sphere’s surface(see Fig. 2). $\bar{\mu}_s$ and σ_{μ_s} are the mean and width of the distribution of static friction coefficient of gently contacting spheres in fluid (see Fig. 5).

sphere material	diameter/ cm	density/($g\text{ cm}^{-3}$)	polydispersity	asphericity	RMS roughness/ μm	$\bar{\mu}_s$	σ_{μ_s}
PTFE	0.3205(4)	2.1389(9)	$0.21 \pm 0.06\%$	$0.14 \pm 0.06\%$	1.1 ± 0.6	0.540 ± 0.003	0.10
aluminum	0.3191(3)	2.775(3)	$\leq 0.04\%$	$\leq 0.04\%$	0.32 ± 0.14	0.62 ± 0.06	0.16
steel	0.3179(4)	7.774(7)	$0.14 \pm 0.05\%$	$\leq 0.04\%$	0.10 ± 0.02	0.66 ± 0.14	0.15
smooth acrylic	0.3174(3)	1.1800(9)	$0.15 \pm 0.06\%$	$0.06 \pm 0.04\%$	0.7 ± 0.3	0.88 ± 0.03	0.10
etched acrylic	0.3092(3)	1.1741(9)	$0.16 \pm 0.07\%$	$0.08 \pm 0.05\%$	2.6 ± 0.1	0.96 ± 0.03	0.10

that are in the neck. The latter is determined from an image of the topography of the top surface of the particles (inset Fig. 1). All volume fractions reported in this article are subject to the same systematic error in the range $\delta\phi \approx 0.000\text{--}0.002$ due to uncertainties in these volumes and in the volume of the hour glass.

The particles used in our experiments are commercially available spheres of acrylic (PMMA), teflon (PTFE), steel, and aluminum with nominal diameter $d \approx 3.18\text{ mm}$ (see Table II, Fig. 2). We also use acrylic spheres which were roughened by timed etches in acetone. All sets of spheres are very monodisperse and highly spherical with, at worst a deviation from sphericity of $\sim 10^{-3}d$, a surface roughness of the same order, and a polydispersity of double this magnitude. These spheres are much larger than those used by Onoda and Liniger ($0.25 \pm 0.02\text{ mm}$, glass). The advantages of using large spheres are evident: attractive van der Waals forces are negligibly small compared to other forces in the problem and the particles are well characterized and of extremely high sphericity and monodispersity. Thus these experi-

ments represent a better approximation to the idealized packing of hard, monodisperse spheres than previous experiments.

Apart from van der Waals attraction[12], experimental results on the low packing fraction limit are sensitive to other attractive forces of electrostatic and capillary origin. In setting up the apparatus, great care was taken to degas fluids and to introduce the fluid to the spheres slowly to avoid entraining air bubbles which form attractive bridges between poorly wetted surfaces, especially rough ones. Pumping a vacuum on heated, stirred fluids for hours was often insufficient to avoid the appearance of attractive forces between spheres in non-wetting fluids, a phenomenon that has recently been associated with the existence of long-lived[21, 22] nanobubbles capable of exerting forces comparable to gravity for PMMA spheres in our more closely density matched fluids[23]. To avoid this phenomenon, we have used well-wetting fluids when possible and avoided close density matches in poorly-wetting fluids so that the contribution of attractive forces is negligible. Where charg-

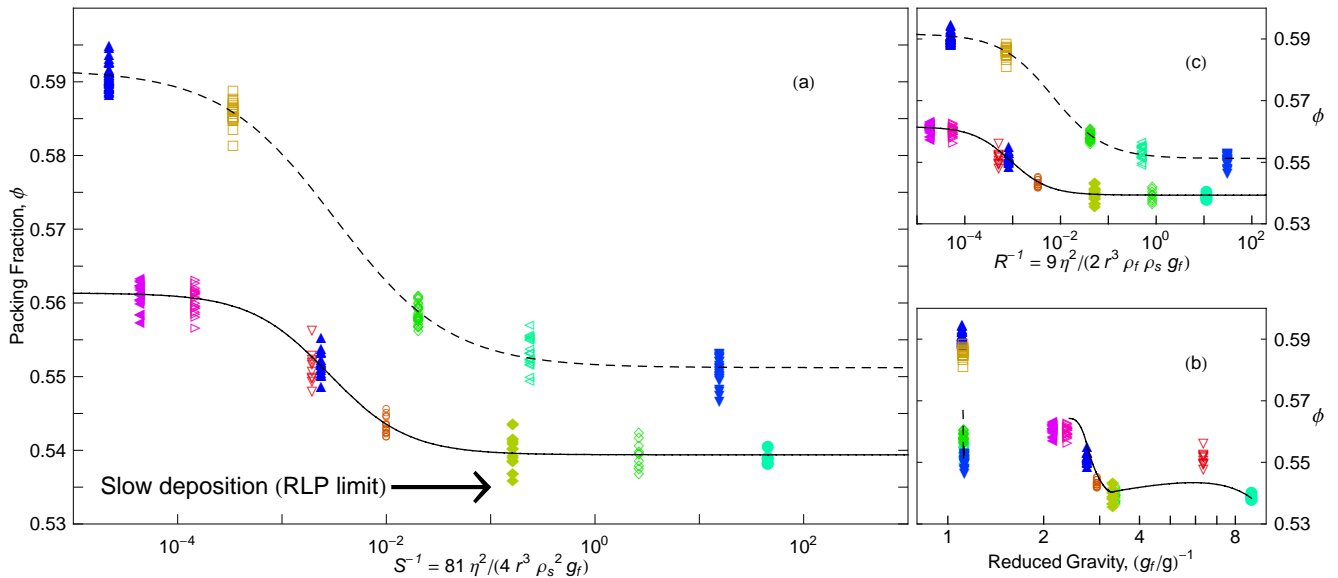


FIG. 3: Packing fraction ϕ vs. the dimensionless parameters S , R , and g_f/g . The data points represent individual packings; the spread in the data is much larger than the random error on each data point. For a particle falling at low Reynolds number, S is the Stokes number and R is the Reynolds number itself. g_f is the buoyancy-reduced gravitational acceleration felt by a particle in the fluid. (Onoda and Liniger’s $\Delta g \equiv g_f/g$ [11].) In all three graphs the solid line connects data for smooth acrylic spheres and the dashed line is for steel spheres.

ing effects were suspected, we repeated measurements with salts added to screen coulomb interactions.

III. RESULTS AND DISCUSSION

The problem of a sphere falling in the fluid involves five dimensionful parameters: $r = d/2$ and ρ_s , the radius and density of the spheres; ρ_f and η , the density and dynamic viscosity of the fluid; and $g_f = g(1 - \rho_f/\rho_s)$, the buoyancy-reduced gravitational acceleration in the fluid. Apart from g_f/g (as suggested by Ref. [11]), other pertinent dimensionless groups are the Reynolds number $Re = 2\rho_f V r/\eta$ and the Stokes number $St = (2/9)\rho_s V r/\eta$, where V is the velocity of the particles as they approach the packing. In reducing our data we use for V , the terminal velocity of the particle under Stokes drag, leading to the dimensionless parameters $R = (2/9)r^3\rho_s\rho_f g_f/\eta^2$ and $S = (4/81)r^3\rho_s^2 g_f/\eta^2$. In the limit of gentle deposition, $R = Re$, $S = St$. S can be interpreted either as a dimensionless damping length, or as the ratio of kinetic energy to the potential energy, $mass \times g_f d$, which quantifies the degree to which a falling sphere can rearrange the packing.

We display in Fig. 3 the major result of this paper. For spheres of a given material, the packing fraction decreases as sedimentation is done more gently. When plotted against the dimensionless group S , the volume fraction approaches an asymptotic limiting low volume fraction which we may interpret as ϕ_{RLP} . We note the

limiting ϕ_{RLP} is different for spheres of different materials. The asymptotic limit is directly available from the data, and unlike in previous measurements need not be obtained by extrapolation (for which there is no reliable theoretical guideline). Each data point is taken with a different liquid, and not with a chemical series or a dilution series; the smooth approach to this limit thus suggests that the macroscopic parameters of the fluid and sphere are sufficient to fully characterize the preparation process, and that any microscopic interparticle interactions mediated by the fluid have been successfully suppressed.

Furthermore, Fig. 3(b) shows that the degree of density matching, quantified by $g_f/g = 1 - \rho_f/\rho_s$, is not an appropriate parameter to define the RLP limit of this packing protocol. Low packing fractions can be achieved without density matching, by sedimenting in sufficiently viscous fluids. For a fluid of a given viscosity, RLP can of course be approached by varying g_f/g , as the work of Onoda and Liniger suggests. The role of g_f/g is however, not in reducing the static load on the packing structure, but purely in slowing down the dynamics of the packing process.

Fig. 3(c) shows that the volume fraction ϕ also smoothly approaches ϕ_{RLP} when plotted against the dimensionless group R . However, unlike the plot of ϕ vs. S , the asymptotic limit is attained at different values of R for different materials, leading us to prefer S as the best candidate for the relevant control parameter.

Additionally, previous measurements of collisions of

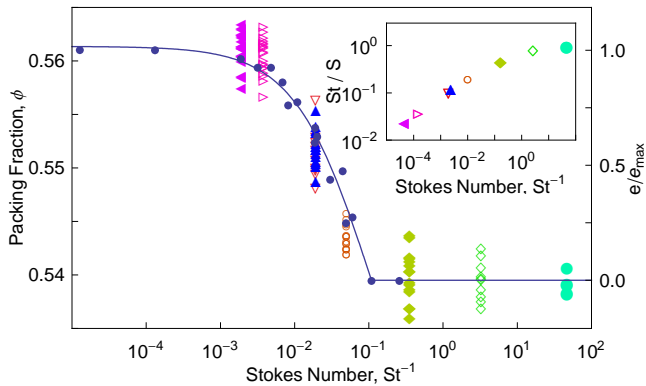


FIG. 4: The main plot shows the packing fraction, ϕ , of acrylic spheres (left vertical axis, symbols match Fig. 3) versus Stokes number, St . We compare the trend with the data of Gondret *et al.* (from Fig. 6, Ref. [24]), plotted here in dark circles against the right vertical axis) for the St -dependence of the restitution coefficient e , scaled by its maximal value e_{max} . The data are for collisions of a teflon sphere in a fluid, however, data for different materials collapse on the same curve. To make the comparison with Ref. [24], we inferred the value of St in our experiments from measured values (Table II) and a standard drag curve[25]. This correction is shown in the inset; as expected the correction is small when St is small.

fluid-immersed spheres on surfaces[24] also show that the Stokes number St – and not Reynolds number Re – is the relevant dimensionless parameter that defines the onset of bounce-free collisions. In addition to supporting the physical picture that the RLP limit corresponds to conditions where sequentially added spheres settle in the first mechanically stable location that they encounter, there is good quantitative agreement between the scale of St where bouncing ceases, and where ϕ_{RLP} is attained. This correspondence is shown in Fig. 4. The Stokes number has also been identified as the parameter controlling the behavior of avalanches in fluid-immersed piles[26].

We now return to the observation that the two curves in Fig. 3 corresponding to steel and acrylic spheres approach different values of ϕ_{RLP} of 0.551 and 0.540 respectively. With the mass density of the materials already accounted for, the only relevant differences are those of the contact mechanics of the spheres. In particular, the effective coefficient of static friction μ_s between spheres is different for these materials. Thus, unlike the RCP limit, the RLP limit is not a purely geometric problem, but involves the mechanics of interactions.

In order to more fully explore this observation, we have prepared packings of five different materials (Table II) in the $St \rightarrow 0$ limit. The coefficient of static friction, μ_s is affected both by material as well as by surface topography; indeed we find that ϕ_{RLP} does not show a simple trend with surface roughness. To directly probe the material property of interest, we have devised a method to measure μ_s for sphere-on-sphere contacts

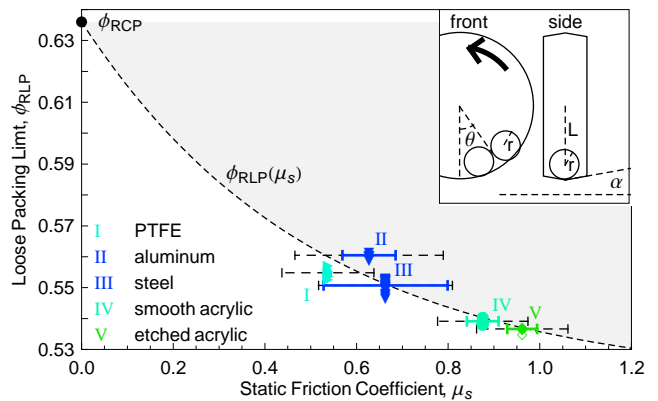


FIG. 5: Limiting low packing fraction ϕ_{RLP} plotted versus μ_s , the mean static friction coefficient. μ_s is measured by a new technique where the friction between spheres immersed in a fluid is ascertained from the maximum angle at which pairs of spheres in a vertical, circular track maintain contact due to static friction. The dashed error bars indicate the width in the distribution of μ_s , and the solid error bars are uncertainty in the mean of μ_s . The shaded area represents the region of stable, disordered packings. The lower bound (dashed curve) is a guide to the eye. The inset shows a drawing of the geometry used in the friction measurement (scale: bead radius $r = 1.59 \text{ mm}$).

between spheres immersed in a liquid. The schematic diagram inset in Fig. 5 shows the geometry of the setup: two spheres sit under gravity in the shallow v-groove of a track in the vertical plane. As the track rotates slowly, static friction between beads prevents them from rolling so they move with the track until they reach a maximal angle θ_{max} . At θ_{max} the tangential force between the spheres exceeds the maximum value allowed by the finite coefficient of static friction μ_s and the beads roll to a lower angle $\theta_{min} < \theta_{max}$. μ_s can be then calculated from θ_{max} [27]. In Fig. 5 we show ϕ_{RLP} decreases monotonically as the measured friction coefficient increases. The dependence on friction coefficient, $\phi_{RLP}(\mu_s)$, is consistent with $\phi_{RLP} \rightarrow \phi_{RCP}$ as the coefficient of static friction, $\mu_s \rightarrow 0$.

Our measurements of μ_s are made under conditions similar to those in our packing experiments, under the same small loads and fluid environments, and with sphere-on-sphere contacts that allow for both sliding and rolling. We are not aware of any other measurements of interparticle friction in this regime. The values of μ_s we observe are larger than those from our everyday experience at larger normal loads. Our data thus suggest a resolution of the puzzle that friction coefficients in simulated contact mechanics models[16–18] were thought to be surprisingly large in order to achieve volume fractions as low as seen in experiments.

Finally, we turn from the RLP limit to the large Stokes regime. Surprisingly, we see a plateau in the value of ϕ , well separated from the low Stokes limit. The plateau ϕ does not scale simply with friction coefficient μ_s , and

presumably also involves other particle properties such as inelasticity. We speculate that this plateau value may be related to the “critical state” of soil mechanics. The transition from this plateau to ϕ_{RCP} is clearly of interest, but is not easily explored by merely tuning S with fluid parameters.

IV. CONCLUSION

The strengths of our experiments are (i) the extremely well-controlled sphericity and monodispersity of the particles, (ii) detailed characterizations of relevant particles properties such as surface roughness and of friction coefficient under deposition conditions, (iii), broad coverage of fluid parameters, and (iv) employing large enough particles to be well outside the influence of any attractive interactions. Thus our experiments provide the best available approximation to the idealized problem of the packing of monodisperse frictional spheres. Despite our choice of experimental geometry, the relatively small system size in our experiments may introduce wall-effects. It is clear, however, that the values of ϕ_{RLP} obtained by the sequential deposition in our experiment are comparable with those obtained by collective packing schemes[11, 15], and therefore our findings should also be applicable to those packing protocols.

Previous experiments have shown that looser packings

may be prepared if sedimentation is done more gently. Our results strengthen this intuitive expectation in three significant directions. The first is that we arrive at a sharp definition of “gentle” deposition: this limit is governed by the Stokes number, St . The second conclusion is that the RLP limit is achieved at a nonzero threshold value of St , below which particles entering the packing do not have the ability to explore the landscape of deposited particles, or to rearrange it. Finally, since we eliminate the effect of attractive forces by packing at finite values of g_f , we establish the existence of a ϕ_{RLP} for cohesionless spheres.

We also provide the first direct experimental study of the friction-dependence of ϕ_{RLP} by measuring the friction coefficients between particles at small normal loads. Friction stabilizes packings at volume fractions considerably below ϕ_{RCP} . The evolution of a packing from the RLP boundary to the RCP boundary, and the structure and mechanical properties of the intermediate states remain largely unexplored.

V. ACKNOWLEDGMENTS

We acknowledge funding from the NSF through nsf-dmr 0606216 and 0907245, and the use of facilities funded by nsf-mrsec 0820506. We thank C. S. O’Hern for valuable conversations.

-
- [1] G. D. Scott, *Nature*, 1960, **188**, 908–909.
 - [2] J. C. Macrae and W. A. Gray, *Br. J. Appl. Phys.*, 1961, **12**, 164–172.
 - [3] R. Rutgers, *Nature*, 1962, **193**, 465–466.
 - [4] G. D. Scott and D. M. Kilgour, *J. Phys. D: Appl. Phys.*, 1969, **2**, 863–866.
 - [5] P. Chaudhuri, L. Berthier, and S. Sastry, *PRL*, 2010, in press.
 - [6] P. Jalali and M. Li, *J. Chem. Phys.*, 2004, **120**, 1138–1139.
 - [7] S. Torquato, T. M. Truskett and P. G. Debenedetti, *Phys. Rev. Lett.*, 2000, **84**, 2064–2067.
 - [8] G.-J. Gao, J. Bławdziewicz and C. S. O’Hern, *Phys. Rev. E*, 2006, **74**, 061304.
 - [9] R. D. Kamien and A. J. Liu, *Phys. Rev. Lett.*, 2007, **99**, 155501.
 - [10] J. D. Bernal, *Proc. R. Soc. A*, 1964, **280**, 299–322.
 - [11] G. Y. Onoda and E. G. Liniger, *Phys. Rev. Lett.*, 1990, **64**, 2727–2730.
 - [12] K. J. Dong, R. Y. Yang, R. P. Zou and A. B. Yu, *Phys. Rev. Lett.*, 2006, **96**, 145505.
 - [13] D. A. Weitz and M. Oliveria, *PRL*, 1984, **52**, 1433–1436.
 - [14] C. S. O’Hern, S. A. Langer, A. J. Liu and S. R. Nagel, *Phys. Rev. Lett.*, 2002, **88**, 075507.
 - [15] M. Jerkins, M. Schröter, H. L. Swinney, T. J. Senden, M. Saadatfar and T. Aste, *Phys. Rev. Lett.*, 2008, **101**, 018301.
 - [16] Z. P. Zhang, L. F. Liu, Y. D. Yuan and A. B. Yu, *Powder Technol.*, 2001, **116**, 23 – 32.
 - [17] L. E. Silbert, D. Ertas, G. S. Grest, T. C. Halsey and D. Levine, *Phys. Rev. E*, 2002, **65**, 031304.
 - [18] C. Song, P. Wang and H. A. Makse, *Nature*, 2008, **453**, 629–632.
 - [19] M. P. Ciamarra and A. Coniglio, *Phys. Rev. Lett.*, 2008, **101**, 128001.
 - [20] *CRC Handbook of chemistry and physics*, ed. D. R. Lide, CRC Press, Boca Raton, 80th edn., 1999.
 - [21] P. Attard, M. P. Moody and J. W. G. Tyrrell, *Physica A (Amsterdam)*, 2002, **314**, 696 – 705.
 - [22] B. M. Borkent, S. M. Dammer, H. Schönherr, G. J. Vancso and D. Lohse, *Phys. Rev. Lett.*, 2007, **98**, 204502.
 - [23] J. Parker, P. Claesson and P. Attard, *J. Phys. Chem.*, 1994, **98**, 8468–8480.
 - [24] P. Gondret, M. Lance and L. Petit, *Phys. Fluids*, 2002, **14**, 643–652.
 - [25] A. K. Majumder and J. P. Barnwal, *IE (I) Journal-M*, 2004, **85**, 17–19.
 - [26] S. Courrech du Pont, P. Gondret, B. Perrin and M. Rabaud, *Phys. Rev. Lett.*, 2003, **90**, 044301.
 - [27] The rotation rate is set slow enough that viscous and centrifugal forces on the particles are negligible compared to gravity and friction. In this limit, $\mu_s = ((L/r)^2 - 1)/(L/s + 1) \tan(\theta_{max})$ where $s = r \cos(\alpha)$. In our setup, $L = 6.35 \pm 0.03 \text{ mm}$, $r = 1.59 \pm 0.03 \text{ mm}$ and $\alpha = 10.0 \pm 0.5^\circ$. L is the distance from the center of the track to the centers of the spheres whereas the radius of the track at contact with the beads is $L + s$.